Int. J. Electrochem. Sci., 14 **(2019)** 11491 – 11508, doi: 10.20964/2019.12.20

International Journal of ELECTROCHEMICAL SCIENCE
www.electrochemsci.org

Corrosion Protection of Mild Steel by the Synergetic effect of Sodium Dodecylbenzenesulfonates and Zinc Sulfate in Sodium Chloride Solution

I.Ismail[1,*], *M.K. Harun*[1], *M.Z.A. Yahya*[2]

[1] Electrochemical and Corrosion Science Laboratory, Faculty of Applied Science, Universiti Teknologi MARA, 40450 Shah Alam Selangor, Malaysia
[2] Faculty of Defence Science & Technology, Universiti Pertahanan Nasional Malaysia, 57000 Kuala Lumpur, Malaysia
[*]E-mail: ismaliza@lgm.gov.my

Received: 31 June 2019 / *Accepted:* 14 September 2019 / *Published:* 29 October 2019

The corrosion inhibition of sodium dodecylbenzenesulfonates surfactant (SDBS) and SDBS incorporated with various concentrations of zinc sulfate ($ZnSO_4$) on mild steel, in 0.05 M NaCl at 25 ^oC were investigated using the electrochemical impedance spectroscopy (EIS) and polarization measurements. The adsorption behavior of SDBS was investigated through different adsorption isotherms. Characterization of the organic film on mild steel surface was done through the Fourier transform infrared spectroscopy (FTIR) analysis. The EIS results found that the corrosion inhibition efficiency (IE) of SDBS was enhanced in the presence of $ZnSO_4$, showing the maximum value of 96% at mixtures of 200:200 ppm SDBS:$ZnSO_4$. The polarization measurement found that the IE for a similar sample was 95%, which agrees well with the EIS results. The calculated thermodynamic parameter reveals that the adsorption process of SDBS obeys the Langmuir adsorption isotherm with the correlation coefficient, R^2 of 0.996. The calculated free energy of adsorption was -33 kJmol-1 which indicated strong adsorption of SDBS on mild steel surface both through physisorption and chemisorption. The FTIR analysis confirmed the presence of the adsorbed organic film on the mild steel surface.

Keywords: Corrosion, mild steel, inhibitor, surfactant, adsorption

1. INTRODUCTION

Steel has become one of the most critical parts of our lives because of its extensive application of structural use for bridges, buildings, pipelines, road vehicles and trains, and also marine. Besides, steel has also been used in most rubber engineering components as a reinforcing material. However, steel, when exposed to an aggressive environment can rust and cause damage to the structures or

components. To date, various mechanical and chemical treatments have been widely employed to protect steel from corrosion damage. Corrosion inhibitors are widely used to protect metals such as steel corrosion in acid or saline environments, which are an effective, practical and economical option [1-6]. There are various types of inhibitors such as inorganic inhibitors (metal oxidizing to form impervious passive layers), or organic inhibitors (absorbed on metal surfaces by heteroatoms and/or double bonds that form thin barrier protection) has been studied to protect the metal surface from corrosion [4]. In addition to the availability and economic reasons, environmental acceptance also influences the selection of corrosion inhibitors [3]. Therefore, the latest research trend is towards promoting the use of non-toxic, economical, and more environmentally friendly green materials as a corrosion inhibitor [7].

In the presence of organic inhibitors, water molecules on the metal surface are replaced by inhibitors through ionic interaction, as illustrated in equation (1) [8]. As a result, it retards the oxidation and reduction reactions by preventing water and ions from reaching the metal surface [9]. A good adsorption process of inhibitors on the metal surface can be achieved if the interaction between the metal and the inhibitor molecule is higher than the metal and water molecules [10].

$$Org + H_2O_{ads} \rightarrow Org_{ads} + H_2O \quad (1)$$

Where Org is organic inhibitor molecules, and Org_{ads} is adsorbed organic inhibitor molecules. It is known that organic inhibitors will modify the surface energy of the metal. Changes in surface energy may have significant effects on the corrosion process, especially when the modified metal surfaces exposed to acid and saline environments [3, 11-15].

Apart from known organic inhibitors, surfactants have also been used to prevent corrosion reactions on metallic surfaces [2,6,11,12,16]. There are many advantages to using surfactant inhibitors as it shows high inhibition efficiency, low toxicity, and ease of production [17]. Due to its hydrophobic nature, surfactant inhibitors can prevent the diffusion of water from reaching the metal surface. The impression of inhibition by surfactants depends on the chemical structure of the surfactant molecule and its absorption properties on the metal surface. They contain electronegative atoms such as nitrogen, oxygen, and sulfur interact with anodic or cathode sites on metal surfaces, thereby reducing the anodic or cathodic reactions and hence corrosion process [18]. Surfactants can be used alone or in conjunction with other compounds to improve their performance [4,6,13,19-20]. Moreover, it has been reported that the addition of metal cations in surfactant or other organic inhibitors is known to enhance the efficiency of inhibition [2,20-21].

In this work, we investigated the ability of sodium dodecylbenzenesulfonates (SDBS), $ZnSO_4$, and SDBS:$ZnSO_4$ mixtures to protect mild steel substrates from corrosion in 0.05 M NaCl. The evaluation of inhibition performance was carried out through the electrochemical spectroscopy (EIS), potentiodynamic measurements, and the infrared reflection spectra (FTIR). Various adsorption isotherms were used to analyze the adsorption behavior of SDBS on mild steel.

2. EXPERIMENTAL

2.1 Materials

Mild steel substrates with a chemical composition of (wt%) 0.60% Mn, 0.15% C, 0.030% P, 0.035% S and 99.185% Fe were used. The mild steel surface was gradually abraded with emery papers (500, 800, 1200, 2400 grit sizes) before used. The sample was cleaned twice with deionized water and acetone before wiped to dry. Analytical grades of sodium dodecylbenzenesulfonates (SDBS) was obtained from Aldrich, while zinc sulfate ($ZnSO_4$) was supplied by HmBG chemicals, and used as received.

The inhibitor solutions were prepared by dissolving either SDBS or $ZnSO_4$ in 0.05 M NaCl solution and stirred for 15 minutes. The concentrations of SDBS used for the study range from 25 to 500 ppm, while the concentrations of $ZnSO_4$ was in the range of 50 to 300 ppm. In order to provide a mixture of SDBS and $ZnSO_4$ solution, SDBS was first dissolved in sodium chloride solution, followed by $ZnSO_4$ and then stirred for 15 minutes. Deionized water was used to prepare all the solutions. Figure 1 illustrates the molecular structures of SDBS.

2.2. Electrochemical measurements

A conventional three-electrode cell with Ag / AgCl coupled to a Luggin capillary as a reference electrode, a platinum rod as a counter electrode, and a mild steel sample as a working electrode were used. A 1 cm^2 mild steel sample electrode was prepared by embedding it into epoxy resin, leaving an exposed area of 0.054 cm^2. The test solution used was 0.05 M NaCl consisting of $ZnSO_4$, SDBS and the mixture of both compounds. All measurements were taken at 25^oC after one hour of immersion in the test solution. The electrochemical impedance spectroscopy (EIS) was carried out at open circuit potential (OCP) within the frequency range of 10 kHz-20 mHz with AC signals of amplitude 10 mV peak to peak. Otherwise, the polarization was measured from -100mV to +100 mV vs. OCP with a scan rate of 1 mV/s. All electrochemical experiments were conducted using an Autolab potentiostat/galvanostat model PGstat302N. The data were analyzed using the Nova software version 1.11.

2.3. Infrared reflection spectra

The mild steel substrate was immersed for 1 h in 0.05 M NaCl solution containing 200:200 ppm SDBS:$ZnSO_4$. The sample was removed from the solution, dried with air, and then left in a desiccator for 24 hours before subjecting to the FTIR analysis. The ATR spectra on the mild steel surface were recorded using Thermo Nicolet 6700 in the range from 400-4000 cm^{-1}. The corresponding spectral acquisition parameters were 36 times scanning and 4 cm^{-1} resolution.

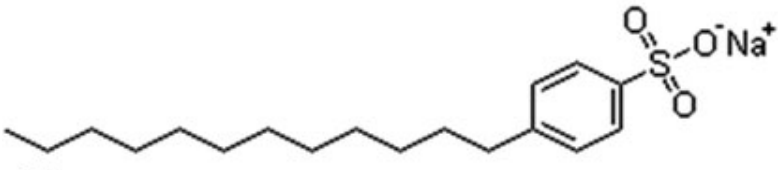

Figure 1. Molecular structure of SDBS

3. RESULTS AND DISCUSSION

3.1 Electrochemical Impedance Spectroscopy (EIS)

Figure 2 illustrates a typical Nyquist and Bode diagrams of a mild steel substrate after immersion for 1 h in 0.05 M NaCl with the absence and presence of SDBS. The EIS measurement exhibits a single depressed semicircle in the Nyquist plot from high to low frequencies which are associated with charge transfer resistance and double-layer capacitance [22-23]. The spectra clearly show a larger diameter of the capacitive loop for the samples immersed in sodium chloride solution in the presence of SDBS compared to the blank solution. The total impedance at low-frequency [Z] 0.02Hz, revealed an ascending trend with increasing SDBS concentrations until a maximum concentration value of 200 ppm. The phase angle values were also found to increase as the frequency moves towards a higher frequency. These results are consistent with the formation of a protective layer on the metal surface caused by the SDBS. As a result, the total resistance towards corrosion of the mild steel was enhanced. However, at much higher concentrations, a reduction in corrosion protection was observed. This was believed to be due to SDBS forming hemi-micelles. Tavakoli et al. (2008), reported a surfactant concentration that goes beyond the critical micelle concentration (CMC), has a thermodynamic tendency to adsorb itself to the bulk solution, thus reducing the amount adsorbed onto the metal surface [24]. Therefore, the maximum inhibition efficiency is determined by the CMC of the surfactant [25].

On the other hand, Figure 3 depicts the Nyquist and Bode diagrams of a mild steel substrate after immersion for 1 h in 0.05 M NaCl solution with and without $ZnSO_4$. The total impedance value at low frequency [Z] 0.02Hz was higher in the presence of $ZnSO_4$ when compared to the blank solution. This indicates that zinc cations reduced the corrosion reactions on the mild steel surface. In addition, there is also an increase in phase angle value at higher frequencies with an increase in $ZnSO_4$ concentration. The combined data indicated an enhanced in the corrosion resistance of mild steel. Similarly, the larger semicircle diameter in the Nyquist plot further demonstrated the effect of significant inhibition on corrosion processes on mild steel surfaces by $ZnSO_4$.

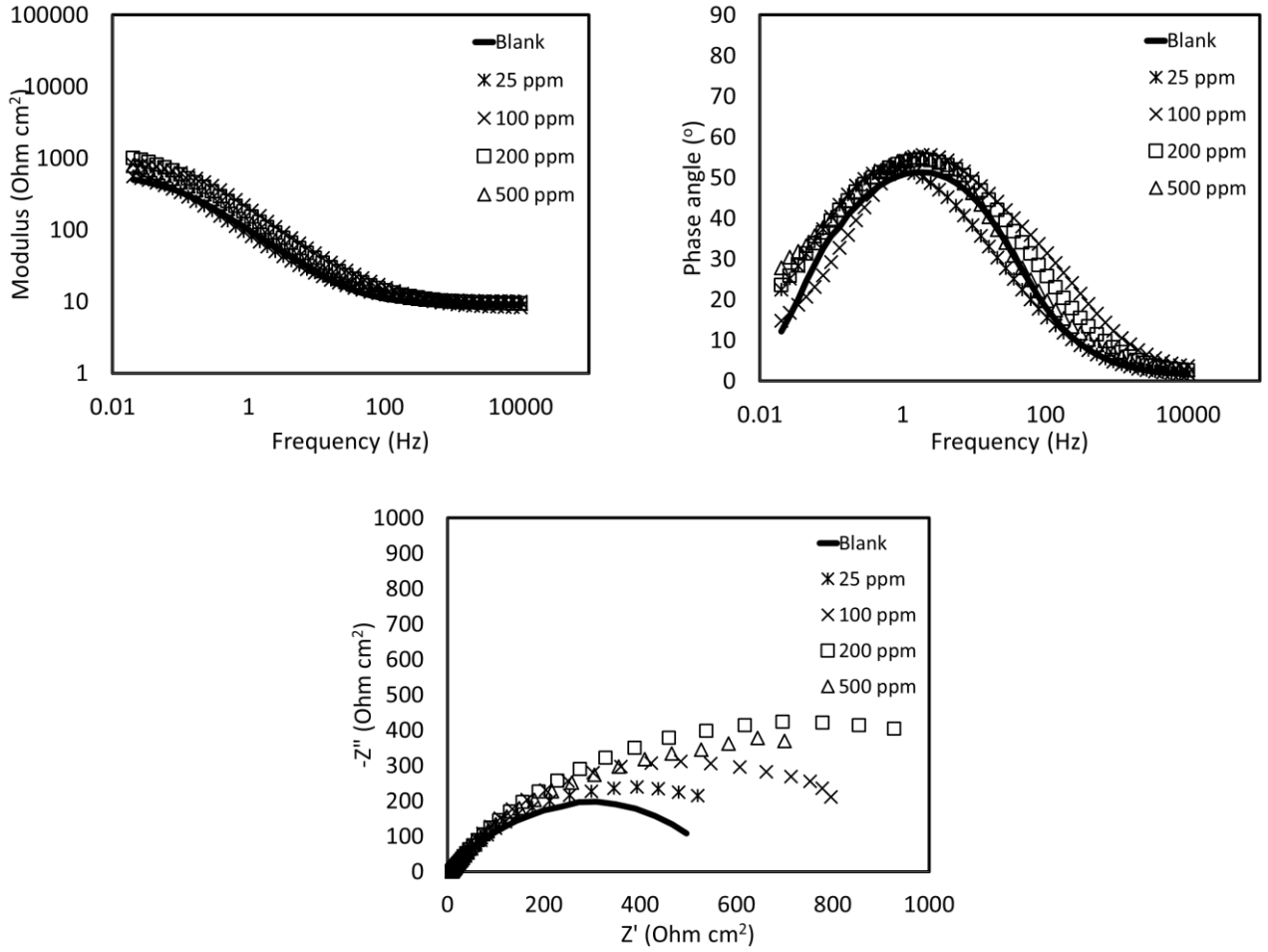

Figure 2. Typical impedance spectra of mild steel substrates after immersion for 1 h in 0.05 M NaCl (a) blank, with SDBS (b) 25 ppm (c) 100 ppm (d) 200 ppm (e) 500 ppm

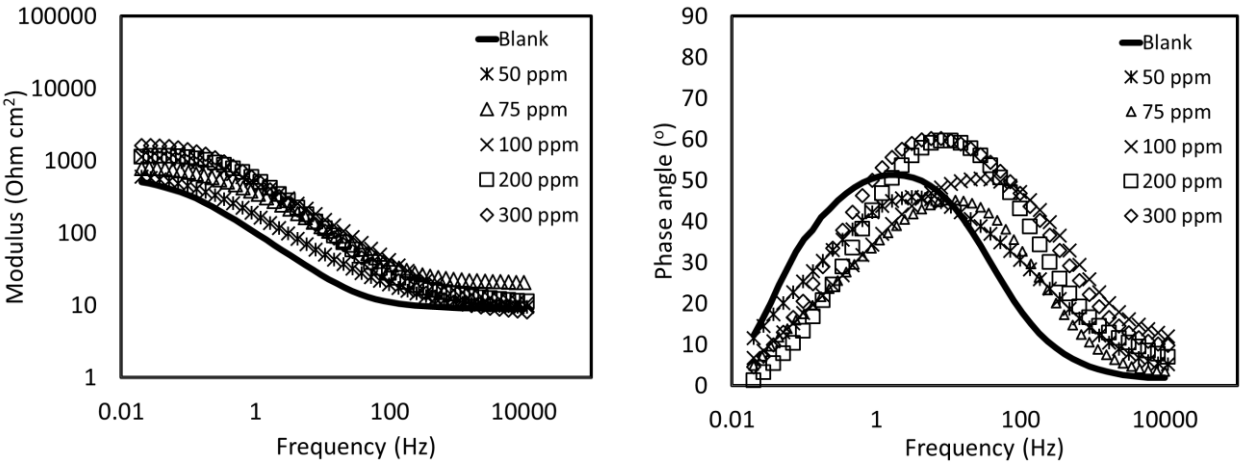

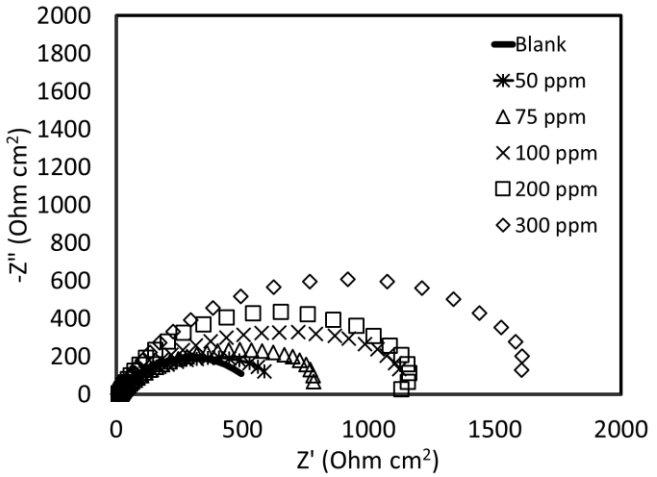

Figure 3. Typical impedance spectra of mild steel substrates after immersion for 1 h in 0.05 M NaCl (a) blank, with $ZnSO_4$ (b) 50 ppm (c) 75 ppm (d) 100 ppm (e) 200 ppm (f) 300 ppm

The synergetic effects of SDBS and $ZnSO_4$ in protecting mild steel corrosion in sodium chloride solutions were investigated. Figure 4 depicts the Nyquist and Bode plots for the mild steel in 0.05 M NaCl solution containing 200:0, 200:75, 200:200, and 200:300 ppm ratio for SDBS:$ZnSO_4$ mixtures. The obtained Nyquist plot shows a larger semicircle diameter when the two inhibitors were mixed. This result indicates a more effective corrosion resistant layer formed when compared to a single inhibitor. In addition, the high impedance values at low frequencies of the Bode's plot confirmed the significant increase in the mild steel resistance towards corrosion. The increasing trend of impedance was observed with increased $ZnSO_4$ concentrations, of which 200 ppm was found to be the most effective. The total impedance for the sample was two magnitudes higher than the blank. Besides, the phase angle plots shifted toward a higher frequency, which also indicates an increase in the total corrosion resistant of the mild steel.

An equivalent electrical circuit (EEC) is proposed to model the experimental data obtained. This is shown in Figure 5. The circuit comprises of R_s, solution resistance, R_{ct}, charge transfer resistance, and $C_{dl,}$ double-layer capacitance. Due to the non-ideal capacitive behavior, a constant phase element (CPE) was introduced instead of using a pure capacitor [22,26]. The relationship between admittance and impedance of CPE are illustrated as follows [22,26]:

$$Y_{CPE} = Y_o(2\pi fj)^n \tag{2}$$

$$Z_{CPE} = Y_o^{-1}(j\omega)^{-n} \tag{3}$$

Where Y_o is admittance, j is the imaginary unit, ω is the angular frequency and n is the CPE power. The value of n is $0 < n \leq 1$ and CPE is a pure capacitor when n is unity.

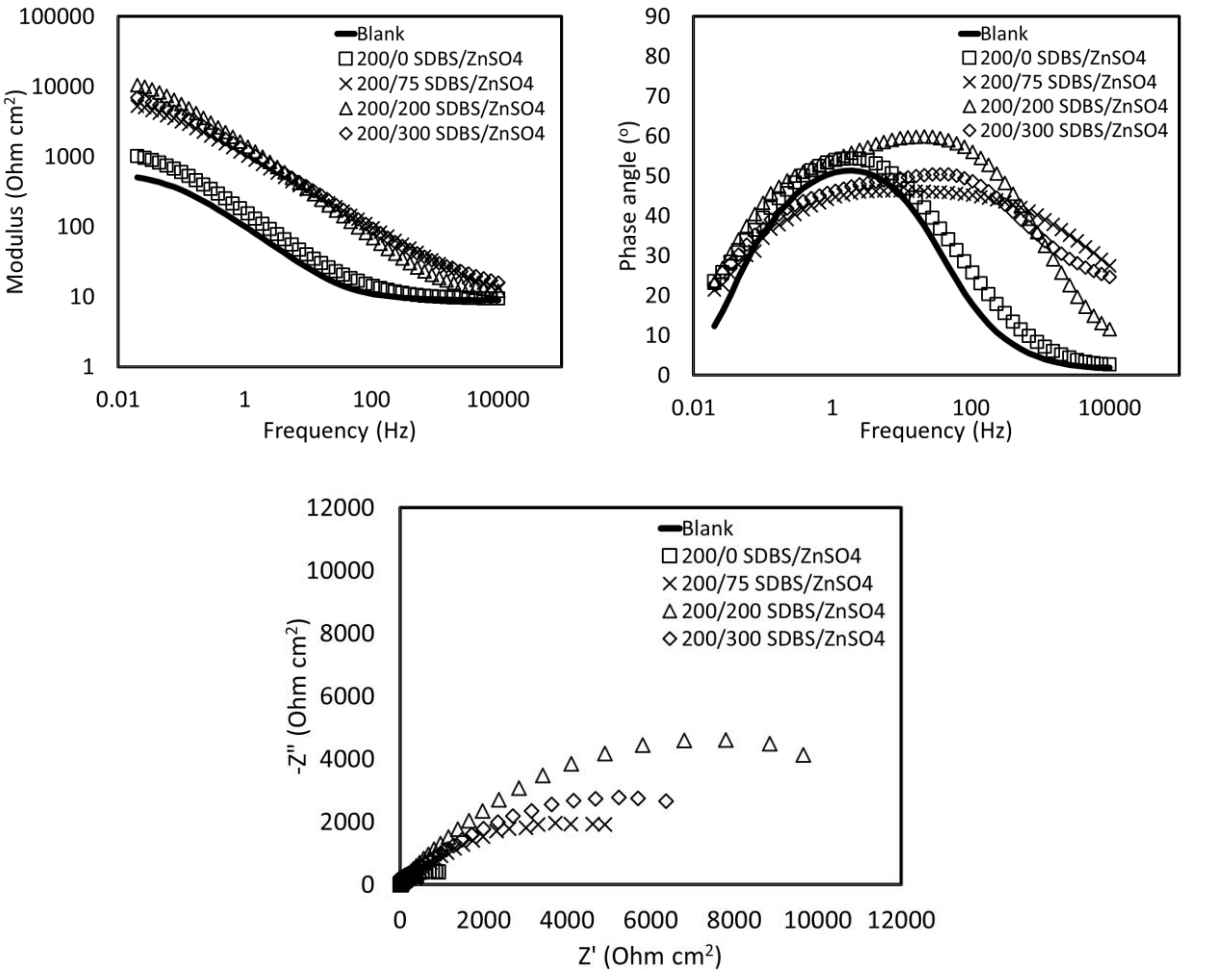

Figure 4. Typical impedance spectra of mild steel substrates after immersion for 1 h in 0.05 M NaCl (a) blank, with SDBS:$ZnSO_4$ mixtures (b) 200:0 ppm (c) 200:75 ppm (d) 200:200 ppm (e) 200:300 ppm

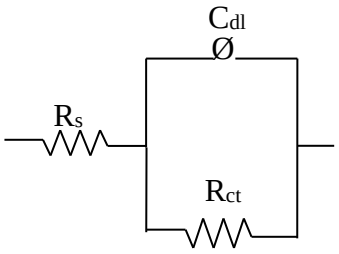

Figure 5. An equivalent electrical circuit used to fit the experimental data

Charge transfer resistance, R_{ct} was used to calculate the inhibition efficiency (η_{EIS}%) as shown in equation (4) [1]:

$$\eta_{EIS} = \frac{R_{ct,i} - R_{ct,o}}{R_{ct,i}} x100 \quad (4)$$

Where $R_{ct,i}$ is the charge transfer resistance with inhibitors and $R_{ct,o}$ is the charge transfer resistances of the blank solution.

Table 1 and Figure 6 show the R_{ct} and η_{EIS} values, respectively, for the mild steel, immersed in sodium chloride solution containing SDBS, $ZnSO_4$, and SDBS:$ZnSO_4$ mixtures. Data fit the equivalent circuit revealed higher R_{ct} values obtained for mild steel immersed in NaCl solution containing either SDBS or $ZnSO_4$ when compared to blank. This indicates that both compounds are able to resist corrosion of the mild steel surface. Although these single compounds are able to resist corrosion, their mixture was found to be more effective. The inhibition effect was also found to be highly dependent on the ratio of SDBS and $ZnSO_4$ mixtures. In this regard, the highest inhibition efficiency was 96% obtained at a ratio of 200:200 ppm SDBS:$ZnSO_4$. Shima Alinejad et. al. (2007) associated this phenomenon to the formation of a good protective coating that prevents electrolyte penetration to the steel surface [1]. At the same time, a significant decrease in C_{dl} values from 175 μF to 15 μF for the blank and mixtures respectively, were obtained. It was speculated that this is due to the water molecules on the mild steel surface that have been replaced by both zinc cations and SDBS molecules which have lower dielectric values [27].

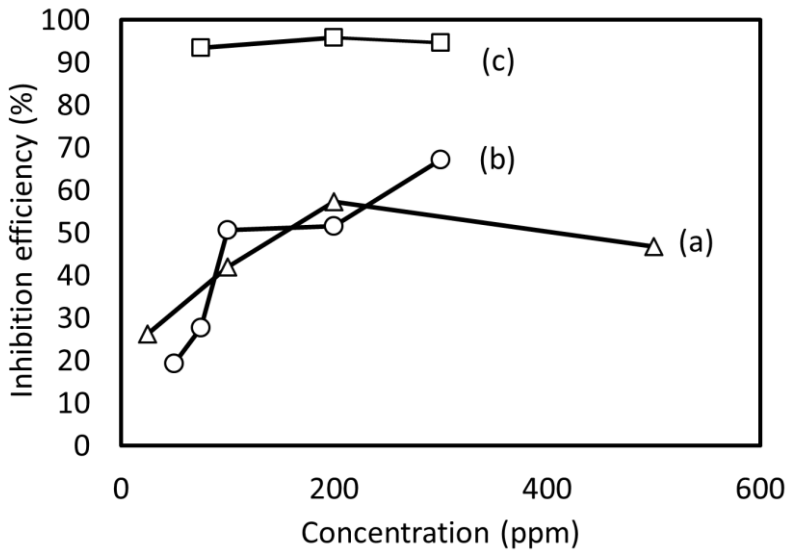

Figure 6. Inhibition efficiency vs concentration of (a) SDBS (b) $ZnSO_4$ (c) Mixture of 200:75, 200:200, 200:300 ppm SDBS:$ZnSO_4$ by EIS measurements

Table 1. EIS measurement of the effects of SDBS and $ZnSO_4$ on steel surfaces after 1-hour immersion in 0.05M NaCl

Concentration (ppm)		R_{ct} (Ohm cm^2)	C_{dl} (μF)	θ	η_{EIS} (%)
SDBS	$ZnSO_4$				
0	0	603	175		-
25	0	817	281	0.26	26.21

100	0	1040	121	0.42	42.03
200	0	1414	140	0.57	57.37
500	0	1133	185	0.47	46.81
0	50	747	102	0.19	19.32
0	75	835	23	0.28	27.77
0	100	1222	17	0.51	50.65
0	200	1246	14	0.52	51.59
0	300	1840	13	0.67	67.23
200	75	9212	40	0.93	93.46
200	200	14688	15	0.96	95.90
200	300	11416	29	0.95	94.72

3.2. Polarization measurements

Polarization measurements were performed on mild steel substrate after immersion for 1 h in 0.05 M NaCl solution in the absence and presence of SDBS, $ZnSO_4$, and a mixture of both compounds. The respective electrochemical parameters of corrosion potential (E_{corr}), corrosion current density (i_{corr}), anodic Tafel slope (β_a) and cathodic Tafel slope (β_c) were calculated and shown in Table 2 [28]. The value of inhibition efficiency (η_{pol}) was calculated using the relation in equation (5) [12]:

$$\eta pol = \frac{i_o - i_i}{i_o} x100 \quad (5)$$

Where i_i is the corrosion current density with the presence of inhibitors and i_o is the corrosion current density for the blank solution.

Figure 7 shows that the E_{corr} of mild steel in sodium chloride solution with SDBS shifted to a more positive value than the E_{corr} of the blank solution, which suggests a decreased of anodic reaction. As a result, it shows that SDBS acts as an anodic inhibitor. As listed in Table 2, the i_{corr} decreased considerably from 21.42 μA cm^{-2} for the blank to 11.83 μA cm^{-2} for the solution with 200 ppm SDBS. The efficiency values obtained were in good agreement with the EIS data. Despite the decrease, however, η_{pol} showed that SDBS did not act as an effective inhibitor with a maximum efficiency of only 48.79% for 200 ppm SDBS obtained [4]. Additionally, there was a reduction in efficiency as the concentration was further increased. As discussed in the EIS study, this behavior might be due to the desorption of inhibitors from the metal surface into the bulk solution which has been associated with CMC [1,12].

On the other hand, Figure 8 depicts the polarization curves of mild steel after immersion for 1 h in 0.05 M NaCl solution with and without $ZnSO_4$. The results show that the addition of zinc cations led to a decrease in the corrosion current density, which is in good agreement with the EIS data [29]. The i_{corr} decreased from 21.42 μA cm^{-2} for the blank solution to a minimum of 5.25 μA cm^{-2} for the solution with 300 ppm $ZnSO_4$ with η_{pol} of 75.5 %. The E_{corr} of the solution with $ZnSO_4$ shifted towards a more negative value than the E_{corr} of the blank solution, indicating a dominant cathodic inhibition mechanism. It can be seen by the naked eye that the white spots on the mild steel surface indicated the formation of insoluble zinc hydroxide/oxide. Zinc hydroxide/oxide deposition was responsible for limiting the rate of

oxygen reduction reactions at active cathodic sites while increasing the corrosion resistance [29]. A significant reduction of βc compared with a blank sample, as shown in Table 2, further indicated the retardation of the oxygen reduction reaction with the presence of $ZnSO_4$.

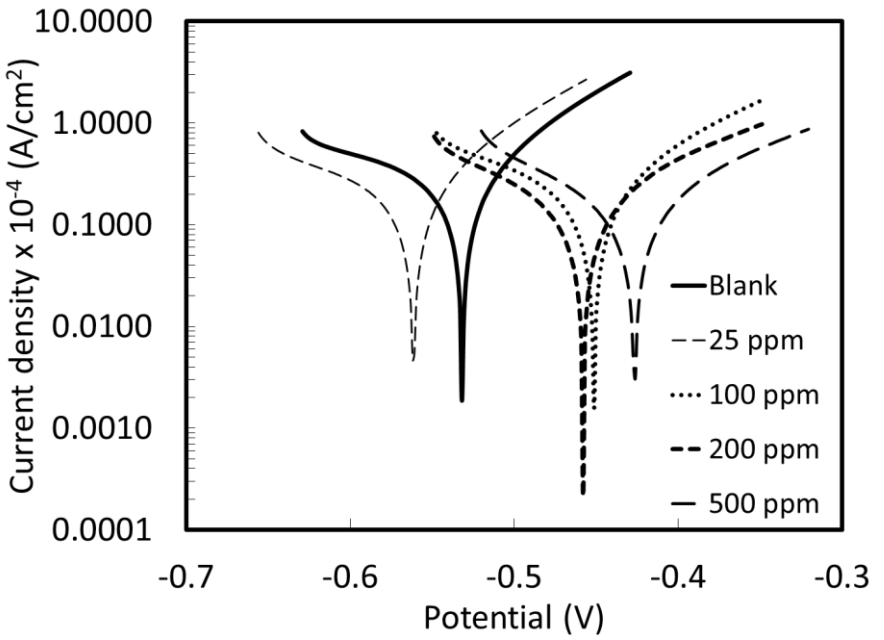

Figure 7. Polarization curves on mild steel immersed for 1 h in 0.05 M NaCl (a) blank , with SDBS (b) 25 ppm (c) 100 ppm (d) 200 ppm and (e) 500 ppm

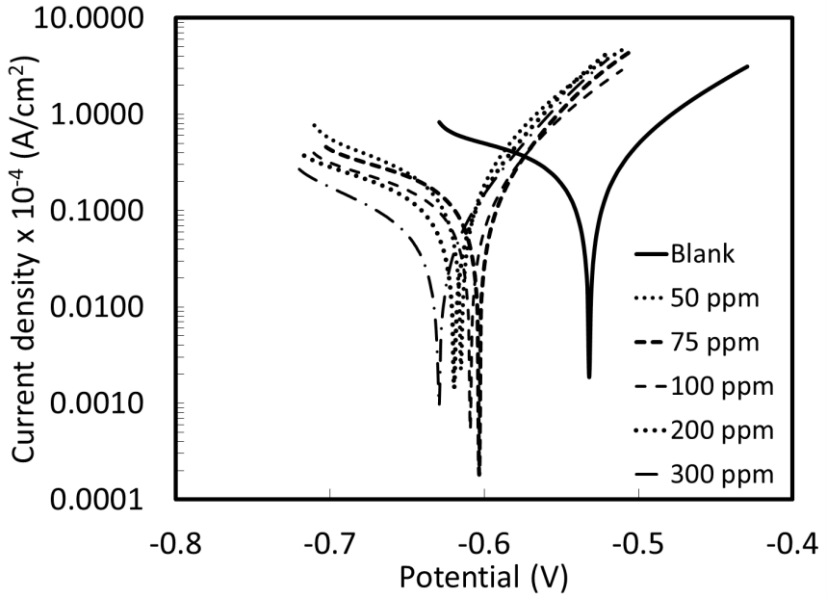

Figure 8. Polarization curves on mild steel immersed for 1 h in 0.05 M NaCl (a) blank , with $ZnSO_4$ (b) 50 ppm (c) 75 ppm (d) 100 ppm (e) 200 ppm and (f) 300

Figure 9 depicts the polarization curves on mild steel substrate after immersion for 1 h in 0.05 M NaCl, and 0.05 M NaCl added with 200:0, 200:75, 200:200 and 200:300 ppm SDBS:$ZnSO_4$. Significant reductions in i_{corr} values were observed for the sample immersed in a solution consisting of both inhibitors compared to the blank solution indicating the formation of a good protective layer. This result agrees well with the charge transfer resistance data from the EIS measurements. The E_{corr} of the mixed inhibitor was slightly shifted in the positive direction compared to the E_{corr} of the blank sample. The shifting was less than 85 mV confirmed that the mixed compound acts as a mixed-type corrosion inhibitor which blocks both anodic and cathodic reactions [30-31]. However, the cathodic curves were nearly overlapped and the anodic curves were in line with the others at different $ZnSO_4$ concentrations. This indicates that the corrosion process was dominantly controlled by the reduction of the anodic reaction [30]. As a result, the SDBS-$ZnSO_4$ mixture prevented the anodic dissolution of the mild steel, thereby reducing the oxygen reduction reaction [32].

The anticorrosion behavior of the protective coating can also be determined by its porosity value. In this case, the porosity of the protective layer formed on the mild steel surface in the presence of inhibitors was calculated from the polarization measurements using equation (6) [33-34]:

$$P = \frac{R_{cto}}{R_{cti}} \, x \, 10^{-(|\Delta E_{corr}|/\beta_a)} \tag{6}$$

Where P is porosity, R_{cto} and R_{cti} are the charge transfer resistance for the blank solution and the solution with inhibitors respectively. ΔE_{corr} is the corrosion potentials difference, and β_a is the anodic slope for the blank solution. The porosity calculated for different samples were listed in Table 2. It was found that the porosity for the single SDBS and $ZnSO_4$ containing solutions are above 70% and 45% respectively, which indicated a porous layer. In this case, water will easily penetrate the coating, thereby reducing the corrosion resistance on mild steel. Instead, the porosity was reduced to a minimum of 9% for the 200:200 ppm SDBS:$ZnSO_4$ mixture, showing that a dense layer was formed on the mild steel surface leading to higher corrosion protection. The results were supported by impedance measurements, where dense layers with high R_{ct} and low C_{dl} were formed for 200:200 SDBS:$ZnSO_4$ compared to $ZnSO_4$ alone. The results obtained in the EIS experiment (Table 1) indicated no significant difference in C_{dl} value was obtained for the 200:200 SDBS:$ZnSO_4$ system when compared to the single $ZnSO_4$, although the R_{ct} was significantly increased. Clearly, in the presence of both inhibitors, it is proposed that $ZnSO_4$ increased the ionic properties of the protective layer thus resulting in the reduced C_{dl} value. The high R_{ct} values obtained are associated with the high corrosion resistant reaction of the stable zinc oxide/hydroxide compound combined with SDBS covering the porous areas. This is consistent with the reduced value on porosity, P, as obtained from Table 2.

It was found that the maximum η_{pol} was 95% for the 200:200 ppm SDBS:$ZnSO_4$. The inhibition efficiency is illustrated in Figure 10. As seen from the EIS measurements, the high efficiency of the mixed inhibitor indicated the formation of a good protective coating that prevents corrosion reaction. Significant reductions in the corrosion current density with slight variations in E_{corr} stated that the protective layer has been able to reduce corrosion by reducing both reaction areas and altering the activation energy for cathodic or anodic reactions [12]. As previously discussed, the rate of cathodic

reaction decreased due to the deposition of zinc hydroxide at the cathodic region, while the adsorption of Zn^{2+} cation and SDBS complex inhibited both anodic and cathodic reactions [1,29]. In this case, SDBS with non-polar chains can reduce water diffusion and its complex with Zn^{2+} improved corrosion resistance [34]. This finding was consistent with earlier reports that metal cations can increase the tendency of organic molecules to prevent corrosion in neutral pH solutions [1].

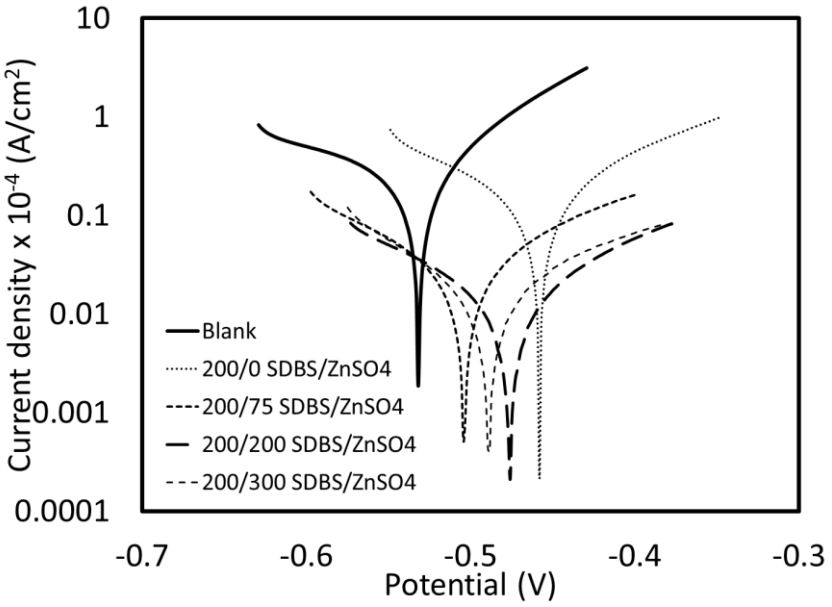

Figure 9. Polarization curves for mild steel substrates after immersion for 1 h in 0.05 M NaCl (a) blank, with SDBS-$ZnSO_4$ mixtures (b) 200:0 ppm (c) 200:75 ppm (d) 200:200 ppm (e) 200:300 ppm

Table 2. Influence of the SDBS and $ZnSO_4$ on the polarization measurements of mild steel after immersion for 1 h in 0.05 M NaCl

Concentration (ppm)		β_a (mV/dec)	β_c (mV/dec)	E_{corr} (V)	i_c ($\mu A/cm^2$)	θ	η_{pol} (%)	P (%)
SDBS	$ZnSO_4$							
0	0	110	219	-0.532	21.42	-	-	-
25	0	84	158	-0.561	16.81	0.22	22	105
100	0	91	132	-0.452	15.33	0.28	28	97
200	0	90	118	-0.458	10.76	0.50	50	72
500	0	116	115	-0.427	11.83	0.45	45	70
0	50	67	190	-0.615	16.96	0.21	21	117
0	75	63	190	-0.603	13.76	0.36	36	99
0	100	64	196	-0.609	10.81	0.50	50	76
0	200	58	178	-0.619	10.20	0.52	52	80
0	300	58	125	-0.630	5.25	0.75	76	45
200	75	88	83	-0.504	2.28	0.89	89	18
200	200	72	89	-0.476	1.07	0.95	95	9
200	300	76	83	-0.489	1.10	0.95	95	10

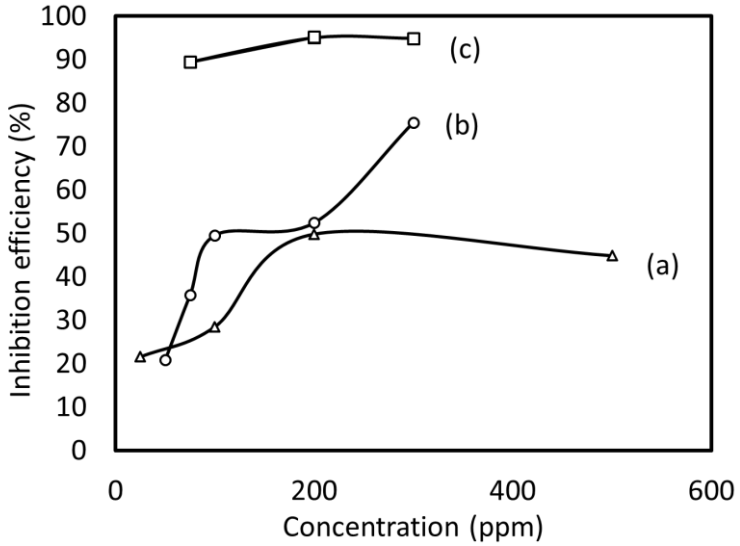

Figure 10. Inhibition efficiency vs concentration of (a) SDBS (b) $ZnSO_4$ (c) Mixture of 200:75, 200:200, 200:300 ppm SDBS:$ZnSO_4$ by polarization measurements

3.3 Synergetic effect

The synergetic effects between SDBS and $ZnSO_4$ were evaluated by estimating the synergy parameter, S_1 calculated using equation (7) as proposed by Aramaki and Hackerman [35] and agreed by other researchers [36-38].

$$S_1 = \frac{1-\theta_{1+2}}{1-\theta r_{1+2}} \quad (7)$$

Where $\theta_{1+2} = (\theta_1+\theta_2) - (\theta_1\theta_2)$, θ_1 is surface coverage of SDBS, θ_2 is surface coverage of $ZnSO_4$ and θ'_{1+2} is surface coverage of SDBS combined with $ZnSO_4$ as obtained from the experimental value in Table 1. A value of $S_1 > 1$ indicates a synergetic effect. This implies that the presence of $ZnSO_4$ facilitated the adsorption of SDBS on the surface [36,38]. Aramaki et al. proposed two kinds of adsorption mechanisms when two compounds are applied onto the metal surface, the competitive and cooperative effects [39]. In the competitive adsorption, the two compounds compete against each other for adsorption and are adsorbed at different sites on the metal surface which causes the antagonistic effects. On the contrary, the cooperative adsorption occurs when both compounds are adsorbed in the same area on the metal surface or the first layer formed. The values of S_1 for the SDBS:$ZnSO_4$ mixture were calculated, and the results are shown in Table 3. All values obtained are greater than the unity showing synergistic effects of the SDBS:$ZnSO_4$ mixtures, indicating a cooperative adsorption mechanism [40].

Table 3 Synergy parameters (S_1) for different SDBS-$ZnSO_4$ concentrations calculated from the EIS measurement

Concentration (ppm)		Synergism parameter (S_1)
SDBS	$ZnSO_4$	
200	75	4.71
200	200	5.03
200	300	2.65

3.4 Critical micelle concentration (CMC) determination

In this study, CMC was determined by plotting $1/i_{corr}$, versus the logarithm of SDBS concentration in accordance with Fuchs-Godec [41]. The plot is shown in Figure 11, and the value is given in Table 4. SDBS molecules comprise both hydrophobic and hydrophilic groups which tend to aggregate at the solution interface and move towards the metal surface between water molecules. The surfactant molecules diffused toward the metal surface continuously resulting in a decrease in the current density [32]. Figure 11 shows a gradual reduction in the current density until the CMC point at 200 ppm SDBS. Beyond this stage, the current density is relatively constant due to the formation of various dimers and aggregates in the solution [32,42]

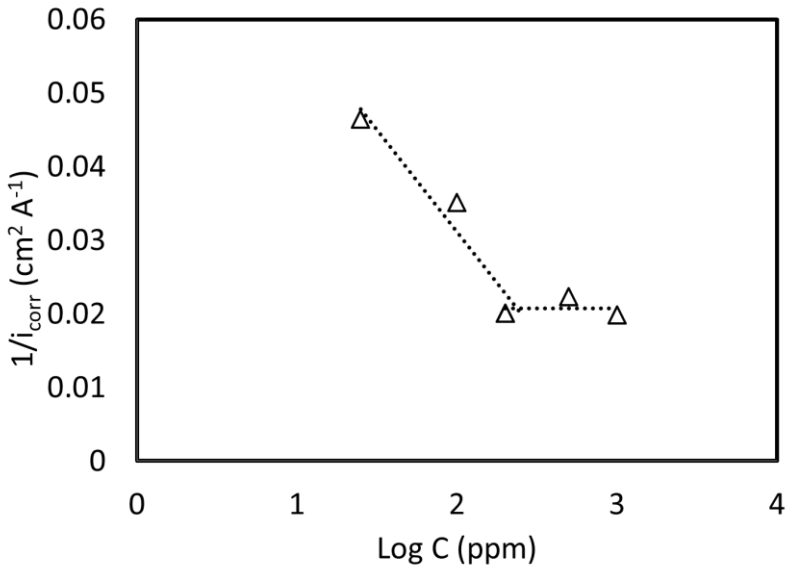

Figure 11. Corrosion current density as a function of SDBS concentration

Table 4 The value of CMC deduced from polarization measurement

Plot	CMC (ppm)
I_{corr} vs. C	200

3.5 Adsorption isotherms

Langmuir adsorption isotherm was used to infer the formation of complex layers on metal surfaces either by physisorption or chemisorption [10]. The surface coverage (θ) and the concentration (C) relationship were used to calculate the adsorption isotherm as shown in equation (9) [43]:

$$\frac{C}{\theta} = \frac{1}{k_{ads}} + C \tag{9}$$

Where k_{ads} is the equilibrium constant of adsorption. The correlation coefficient R^2 obtained for SDBS is 0.996, indicating that the adsorption of SDBS on the steel surface corresponds to the Langmuir adsorption model, as shown in Figure 12. The free energy of adsorption ΔG_{ads}^{o} was calculated by equation (10) [12].

$$\Delta G_{ads}^{o} = -RTLn(55.5k_{ads}) \tag{10}$$

Where, gas molar constant, R is 8.314 J $(K\ mol)^{-1}$, Temperature, T in K [12].

The electrostatic interactions between molecules and metal surfaces were inferred when ΔG_{ads}^{o} is less than -20 kJ mol^{-1}, indicating that the adsorption is through physisorption. While the chemisorption process occurs if ΔG_{ads}^{o} greater than −40 kJ mol^{-1} suggesting that a chemical interaction exists between the adsorption molecule and the metal surface [10,12,44]. In this experiment, it was found that ΔG_{ads}^{o} is −33 kJ mol^{-1}, concluding that both physisorption and chemisorption processes took place between the SDBS molecules and the mild steel surface.

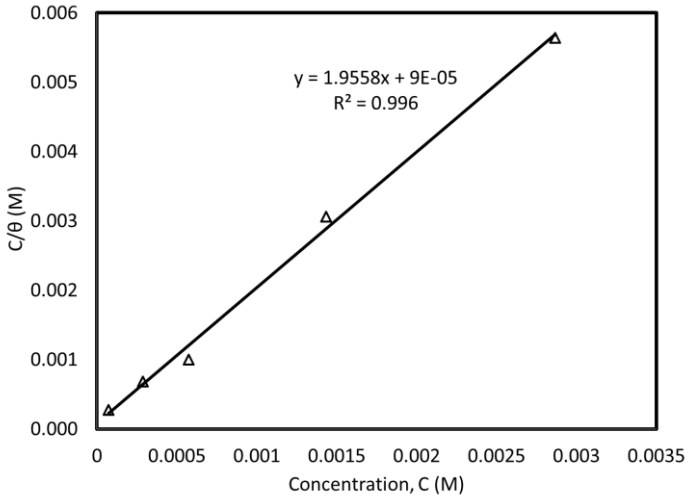

Figure 12. Langmuir adsorption isotherm of SDBS on mild steel surface derived from EIS measurement.

3.6. Infrared reflection spectra

Figure 13 shows the ATR results on a mild steel surface after immersion for 1 h in 0.05 M NaCl solution containing 200:200 ppm SDBS:$ZnSO_4$. Band at 1166 cm^{-1}, 1035 cm^{-1}, 680 cm-1 indicated the $-SO3^{-}$ stretching vibrations and band at 1631 cm^{-1}, 1454 cm^{-1} indicated the C=C vibration suggesting the

formation of $Fe(SDBS)_2$ complex [2,25]. The formation of this complex was believed to have enhanced the corrosion protection of mild steel in sodium chloride solution as obtained in the electrochemical measurements.

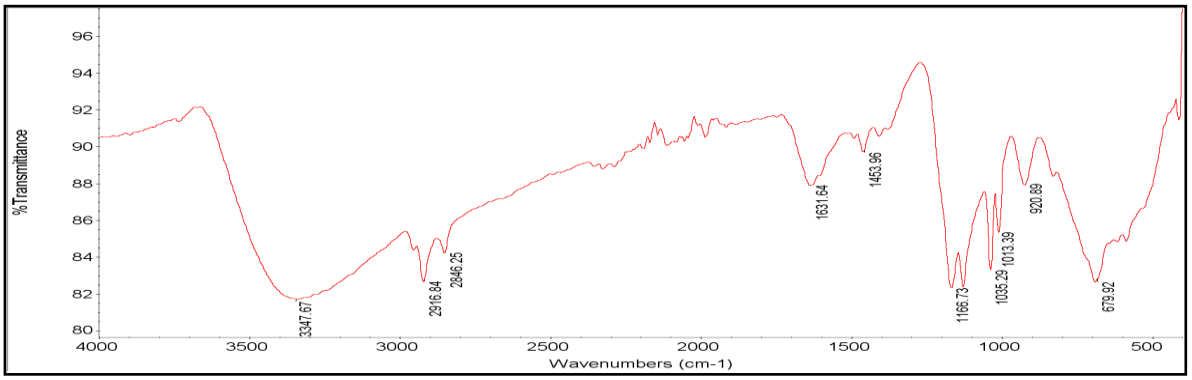

Figure 13. FTIR-ATR spectra on mild steel surface after immersion for 1 h in 0.05 M NaCl solution containing 200-200 ppm of SDBS-$ZnSO_4$

4. CONCLUSION

Although SDBS does not act as an efficient corrosion inhibitor by itself, the SDBS:$ZnSO_4$ system was found to perform a better corrosion protection layer on a mild steel substrate in 0.05 M NaCl solution as obtained through the polarization and EIS measurements. The inhibition efficiency was ~96% for 200:200 ppm SDBS:$ZnSO_4$. The corrosion protection efficiency affected the porosity of the protection layer formed on the steel surface. It was found that both the effects of passivation and barrier contributed to the total increase in corrosion protection. The formation of zinc oxide and zinc hydroxide together with the non-polar chains of SDBS prevents the diffusion of water and ions to the steel surface, thereby increasing the corrosion resistance. Thermodynamic studies concluded that the adsorption of SDBS on metal surfaces follows the Langmuir isotherm with free energy adsorption of -33 kJ mol^{-1}. This result suggests that the adsorption of SDBS was both through physisorption and chemisorption. The FTIR analysis confirmed the presence of the SDBS compound.

ACKNOWLEDGMENT

The author would like to thank the Faculty of Applied Sciences, Universiti Teknologi MARA for permitting to publish this paper and the Malaysian Rubber Board for their technical support of the tasks. Lastly, immense gratitude to the Fundamental Research Grant Scheme, Malaysian Ministry of Education for funding this research work.

References

1. S. Alinejad, R. Naderi, and M. Mahdavian, *J. Ind. Eng. Chem.*, 48 (2017) 88.
2. J. Liu, D. Wang, L. Gao, and D. Zhang, *Appl. Surf. Sci.*, 389 (2016) 369.
3. M. Mobin, and M.A. Khan, *J. Mater. Eng. Perform.* , 23(2014), 222.
4. S.A. Umoren and M.M. Solomon, *J. Environ. Chem. Eng.*, 5 (2017) 246.

5. D. Wang, D. Yang, D. Zhang, K. Li, L. Gao, and T. Lin, *Appl. Surf. Sci.*, 357 (2015) 2176.
6. B. Zhou, Y. Wang and Y. Zuo, *Appl. Surf. Sci.*, 357 (2015) 735.
7. M. Mobin, M. Parveen, and M. Rafiquee, *Arab. J. Chem*, 10 (2017), S1364.
8. K. Hu, J. Zhuang, J. Ding, Z. Ma, F. Wang, and X. Zeng, *Corros. Sci., 125 (2017)*, 68.
9. A.M. Badawi, M.A. Hegazy, A.A. El-Sawy, H.M. Ahmed and W.M. Kamel, *Mater. Chem. Phys.*, 124 (2010) 458.
10. H. Serrar, M. Galai, F. Benhiba, M. Ouakki, Z. Benzekri, S. Boukhris, A. Hassikou, A. Souizi, H. Oudda, and M.E. Touhami, *J. Chem. Technol. Metall.*, 53 (2018) 597.
11. A. Balbo, A. FRignani, V. Grassi and F. Zucchi, *Corros. Sci.*, 73 (2013) 80.
12. S. Javadian, A. Yousefi, and J. Neshati, *Appl. Surf. Sci.*, 285 (2013) 674.
13. F. Kellou-Kerkouche, A. Benchettara, and S. Amara, *Mater. Chem. Phys 110* (2008), 26.
14. M. Migahed, E. Azzam, and A. Al-Sabagh, *Mater. Chem. Phys.*, 85 (2004) 273.
15. M. Mobin and R. Aslam, *Process Saf. Environ.*, 114 (2018) 279.
16. A. de Oliveira Wanderley Neto, A. Neuma de Castro Dantas, A.A. Dantas Neto, and A. Gurgel, Chapter 19 - Recent Advances on the Use of Surfactant Systems as Inhibitors of Corrosion on Metallic Surfaces, in The Role of Colloidal Systems in Environmental Protection, Elsevier (2014), Amsterdam, Netherlands.
17. R. Mehdaoui, A. Khelifa, and O. Aaboubi, *Res. Chem. Intermediat., 41*(2015), 705.
18. S.A. Ali and M.T. Saeed, *Polymer*, 42 (2001) 2785.
19. M. Mobin, and M.A. Khan, *Chem. Eng. Commun., 200*(2013), 1149.
20. A.L. Rose, A.P.P. Regis, S. Rajendran, A. Krishnaveni and F.R. Selvarani, *Arab J. Sci. Eng.*, 37 (2012) 1313.
21. A. Ghazi, E. Ghasemi, M. Mahdavian, B. Ramezanzadeh and M. Rostami, *Corros. Sci.*, 94 (2015) 207.
22. B. Qian, B. Hou, and M. Zheng, *Corros. Sci.*, 72 (2013) 1.
23. H. Tian, W. Li, A. Liu, X. Gao, P. Han, R. Ding, C. Yang and D. Wang, *Corros. Sci.*, 131 (2018), 1.
24. H. Tavakoli, T. Shahrabi and M. Hosseini, *Mater. Chem. Phys.*, 109 (2008) 281.
25. S.S.A. El Rehim, M.A. Amin, S.O. Moussa and A.S. Ellithy, *Mater. Chem. Phys.*, 112 (2008) 898.
26. I. Ismail, M.K. Harun and M.Z.A. Yahya, *Rubber Chem. Technol.*, 88 (2015) 502.
27. B.A. Rao, M.V. Rao, S.S. Rao and B. Sreedhar, *Chem. Eng. Commun.*, 198 (2011) 1505.
28. M. Yadav, D. Behera, S. Kumar, and R.R. Sinha, *Ind. Eng. Chem. Res, 52*(2013), 6318.
29. S. Alinejad, R. Naderi and M. Mahdavian, *Prog. Org. Coat.*, 101 (2016) 142.
30. K. Cao, H. Sun, X. Zhao and B. Hou, *Int. J. Electrochem. Sci.*, 9 (2014) 8106.
31. H. Tian, W. Li, K. Cao, and B. Hou, *Corros. Sci*., 73 (2013), 281.
32. E. Kowsari, M. Payami, R. Amini, B. Ramezanzadeh, and M. Javanbakht, *Appl. Surf. Sci*., 289 (2014), 478.
33. J. Creus, H. Mazille and H. Idrissi, *Surf. Coat. Tech.*, 130 (2000) 224.
34. S. Chaudhari and P.P. Patil, *Electrochim. Acta*, 55 (2010) 6715.
35. K. Aramaki, and N. Hackerman, *J. Electrochem. Soc., 116* (1969), 568.
36. M. Mobin, S. Zehra, and R. Aslam, *RSC Adv, 6* (2016), 5890.
37. P. Roy, A. Pal, and D. Sukul, *RSC Adv, 4* (2014), 10607.
38. S.A. Umoren, and A. Madhankumar, *J. Mol. Liq.*, 224 (2016), 72.
39. K. Aramaki, M. Hagiwara, and H. Nishihara, H. (1987). The synergistic effect of anions and the ammonium cation on the inhibition of iron corrosion in acid solution. *Corros. Sci., 27* (1987), 487.
40. M. Azaroual, E. El Harrak, R. Touir, A. Rochdi, and M.E. Touhami, *J. Mol. Liq.*, 220 (2016), 549.
41. R. Fuchs-Godec, *Colloids Surf. A*, 280 (2006) 130.
42. A. Kosari, M.H. Moayed, A. Davoodi, R. Parvizi, m. Momen, H. Eshghi and H. Moradi, *Corros. Sci.*, 78 (2014) 138.
43. Y. Qiang, S. Zhang, B. Tan, and S. Chen, *Corros. Sci.*, 133 (2018) 6.

44. J.H. Liu, Z. W. Zhan, M. Yu, and S.M. Li, *Appl. Surf. Sci., 264 (2013)*, 507.